Journal of Magnetics 16(4), 332-336 (2011) http://dx.doi.org/10.4283/JMAG.2011.16.4.332

Effect on N Defect in Cu-doped III-nitride Semiconductors

Byung-Sub Kang*, Jae-Kwang Lee, Yong-Sik Lim, Kie-Moon Song, and Kwang-Pyo Chae

Department of Nano Science and Mechanical Engineering, Konkuk University, Chungju 380-701, Korea

(Received 16 June 2011, Received in final form 14 November 2011, Accepted 13 December 2011)

We studied the effect on the electronic and magnetic properties of the N defect in clean and Cu-doped wurtzite III-nitrides by using the first-principles calculations. When it is doped two Cu atoms in the nearest neighboring sites, the system of AlN, GaN, or InN with the N vacancy is energetically more favorable than that without the N vacancy site. When the Cu concentration increases, the total magnetic moment of a supercell becomes small. The ferromagnetism of Cu atom is very low due to the weak 3*d*-3*d* coupling. It is noticeable that the spin-exchange interaction between the Cu-3*d* and N defect states is important.

Keywords : Cu-doped III-nitrides, nitrogen defect, ferromagnetism

1. Introduction

The transition metal-doped III-nitrides diluted magnetic semiconductors (DMSs) have attracted intense attention because of their potential applications in spintronics devices which utilize both the charge and the spin of electrons to create new functional beyond conventional semiconductors. An ideal DMS should exhibit the ferromagnetism at room temperature for the practical applications and have a homogeneous distribution of the magnetic dopants. However, the formation of clusters or secondary phases between the magnetic dopants and host atoms will have a bad influence on the practical applications. The group III-nitrides AlN, GaN, InN and their alloys have been widely studied both theoretically and experimentally [1-10]. The Cr- and Mn-doped GaN semiconductors are now one of the most extensively studied classes of semiconductor materials. It has been reported that the Cr-doped AlN semiconductor films are ferromagnetic at temperature over 340 K [3]. Chen and coworkers have reported that the homogeneous $In_{0.98}Cr_{0.02}N$ film grown at 300 °C shows the ferromagnetic properties with Curie temperature higher than 350 K [8]. Recently it has been reported that the nonmagnetic dopant Cu in GaN is a promising DMS free of magnetic precipitates [11]. They report that the Cu-doped GaN favors ferromagnetic ground state which can be explained in terms of *p-d* hybridization mechanism, and a Curie temperature around 350 K can be expected.

In the present paper, we studied systematically on the electronic and the magnetic properties for Cu-doped group III-nitrides with a Cu concentration of 6.25-12.5%, as well as the effects on the electronic properties of nitrogen vacancy were considered. The possibility of Cu as a non-magnetic dopant to fabricate DMS based AlN was examined by first-principles calculations. As well known, the defects and the impurities are believed to play important roles in DMSs of wide semiconductor gaps. A recent theoretical study [12, 13] has been confirmed that the nitrogen vacancy should be the dominant defect in GaN in the whole range of Fermi-level positions in the band gap. We aimed to investigate the electronic structures and magnetism under different doping concentrations with (or without) the defect of nitrogen.

2. Calculation Method

The electronic and magnetic properties on the Cu-doped III-nitrides with the Cu concentration of 6.25% and 12.5% had been studied for a supercell of 32 atoms with one or two atoms substituted by Cu (the configuration of Cu site was specified in Fig. 4). The calculations had been performed by using a self-consistent full-potential linear muffin-tin orbital (FP-LMTO) method [14, 15] based on spin density functional theory with the local spin-density approximation (LSDA). The local part of the Wang and Perdew parameterization of the exchange-correlation

*Corresponding author: Tel: +82-43-840-3627
Fax: +82-43-851-4169, e-mail: kangbs@kku.ac.kr

energy was used [16]. The LMTO basis set and the charge density were expanded in terms of the spherical harmonics up to $l = 6$ inside each muffin-tin sphere. The basis functions in the interstitial region were expanded by the smoothed Hankel functions [14]. The valence electrons were not assumed to have the spin-orbit coupling but had generated the self-consistent supercell potential by considering the scalar relativistic effects.

The atomic potentials were approximated by spherically symmetric potential, however the full charge density including all nonspherical terms was evaluated by Fourier transformation in the interstitial region. The charge density was determined self-consistently by using a gamma-centered 4 × 4 × 4 grid in the Brillouin zone. The improved tetrahedron method by Blöchl [17] had been chosen to improve the convergence of the electronic structure and total energy with respect to the number of k points. Using 64 k points insured that the total energy and the magnetic moment converge with an accuracy of 10 meV/cell and 0.01 μ_B/atom, respectively. Broyden [18] and Pulay [19] strategies for charge-density mixing were used to accelerate convergence of charge and spin densities and potentials.

3. Results and Discussion

We found that the calculated equilibrium lattice parameters $a = 3.108$ Å and $c/a = 1.6009$ for the clean AlN. For GaN, they were $a = 3.187$ Å and $c = 5.183$ Å. They were $a = 3.480$ Å and $c = 5.615$ Å for the clean InN. In our calculations, we performed a minimization of the total energy for the supercell volume when keeping the constant c/a ratio. The calculated parameters are in agreement with the experimental and the calculated ones [2, 5, 20-22].

Fig. 1 shows the densities of states (DOS) for the clean AlN, GaN, and InN with the vacancy at nitrogen site (V_N). That is, it is a summation of DOS for Al, Ga, In, and N atoms. It shows the downward shift in energy by 4.2 eV, 2.5 eV, and 1.4 eV for AlN, GaN and InN, respectively, in comparison with complete structures. Filled DOS represents the states of the V_N site. The defect states are not formed in mid bandgap. It is located at the top of valence band (E_v) and the bottom of conduction band. In the case of AlN, it shows the p-type semiconductor character which introduces the acceptor defect-state. As can be seen in Fig. 1, the calculated band gaps of clean AlN, GaN, and InN are 3.7, 2.0, and 1.7 eV, respectively. These results of AlN and GaN are smaller than those of experimental values. On the other hand, for InN, the band gap is larger than the experimental ones. In general, the value of band gap calculated by using the LSDA is less than half of the value obtained in the experiment.

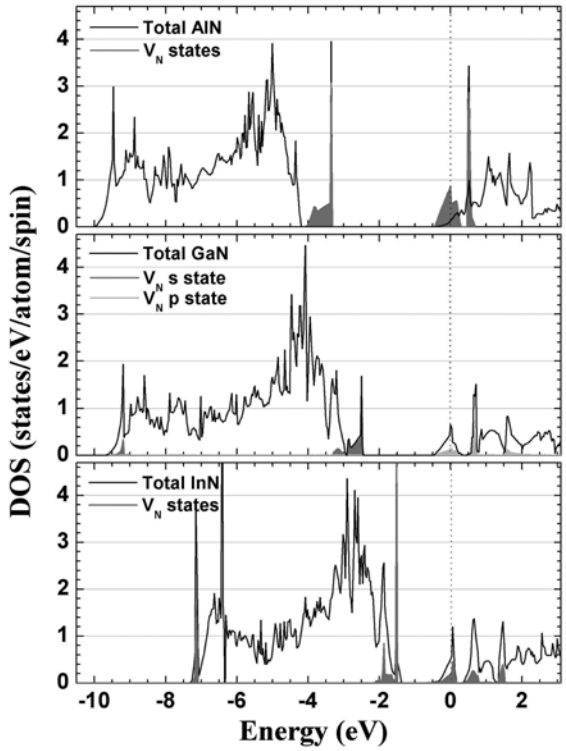

Fig. 1. Total DOS of AlN, GaN, and InN with V_N, Filled gray represents the V_N states. The E_F is set to zero.

Table 1. Formation energy of N vacancy (E_f, in eV), substitution energy (E_s, in eV), and total magnetic moments (M/cell, in μ_B) of supercell for the $X_{0.9375}Cu_{0.0625}N$ (X=Al, Ga, and In) with the N vacancy. The values in the parenthesis represent the magnetic moment of Cu atom.

	AlN	GaN	InN
E_f	−11.413	−8.899	-6.581
E_s	−1.571	−0.594	-0.557
M/cell	0.75(0.43)	0.50(0.25)	0.38(0.19)

Fig. 2(a) and 2(b) illustrate the differences in charge density, Δρ, for the $Al_{0.9375}Cu_{0.0625}N$ and the $In_{0.9375}Cu_{0.0625}N$ with the V_N site in the ground state. The Δρ is defined as ρ(Cu, XN, [V_N]) − ρ(XN, [V_N]) − ρ(1Cu), where ρ(1Cu, XN, [V_N]) is the total charge density, and ρ(XN, [V_N]) and ρ(1Cu) are the charge densities for XN (X=Al and In) without [or with] the V_N and an isolated Cu atom, respectively. The strong interaction between Cu and N atoms occurs due to the charge accumulation among neighboring Cu and N atoms. It shows the profile of moved charge in the site of a vacancy. In the case of AlN, the substitution energy between Cu and Al atoms is the

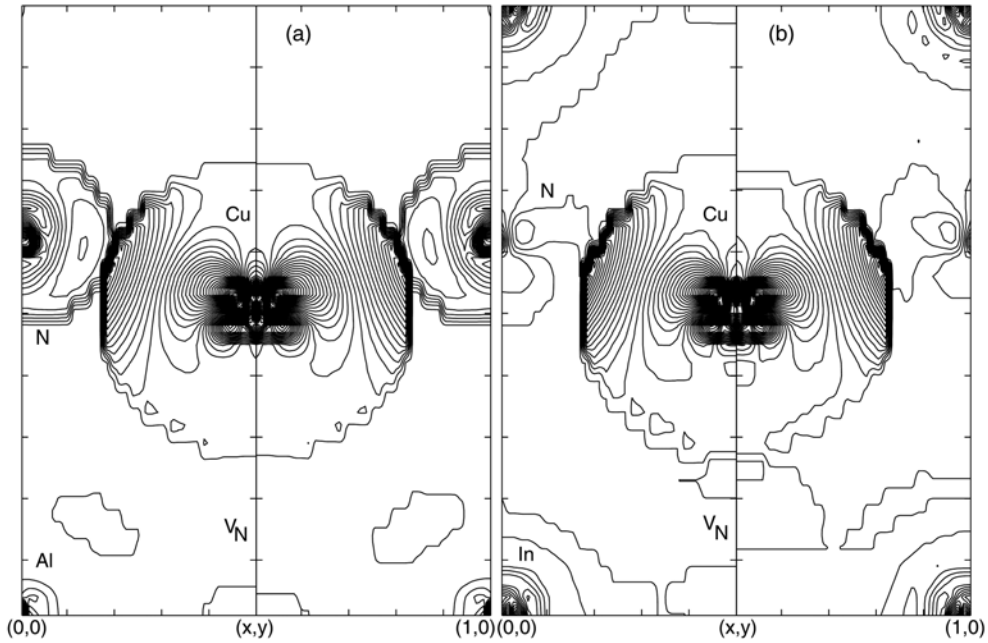

Fig. 2. Charge density difference (Δρ) for (a) the $Al_{0.9375}Cu_{0.0625}N$ and (b) the $In_{0.9375}Cu_{0.0625}N$ with the V_N. The contour is shown on the (11$\underline{2}$0) plane with intervals a 5.0×10^{-4} e/(a.u.)^3. The coordinate (x, y) corresponds to (1/2, 3/6). Here, the lattice parameter is set to 1.

lowest, the vacancy formation energy also is the lowest. These results are listed in Table 1. The vacancy formation energy is defined as $E_{tot}(X, N) - E_{tot}(X, N, V_N) - E_{tot}(N)$. The substitution energies are defined as $(E_{tot}(X, N, [V_N]) - E_{tot}(X)) - (E_{tot}(X, Cu, N, [V_N]) - E_{tot}(Cu))$, where $E_{tot}(X, N, [V_N])$ is the total energy of undoped-XN (X=Al, Ga, and In) with (or without) the V_N, $E_{tot}(X, Cu, N, [V_N])$ is the total energy of Cu-doped system with (or without) the V_N. $E_{tot}(X, N)$ is the total energy of perfect XN without the V_N, $E_{tot}(X)$, $E_{tot}(Cu)$, and $E_{tot}(N)$ are that of an isolated X, Cu and N atoms.

Fig. 3 shows the DOS for $X_{0.9375}Cu_{0.0625}N$ with the V_N site. The N-*2s* states in the group III-nitrides locate around −14 ~ −12 eV. The lowest conduction band and the highest valence band originate mainly from N-2*p* and Cu-3d electrons. Fully occupied dopant states are generated just near the Fermi level (E_F). The E_F is located at the top of the valence band in the case of majority spin-states.

Fig. 4 shows the DOS for $X_{0.875}Cu_{0.125}N$ with the V_N site. We can see that there is the difference in the crystal field splitting of *e* and t_2 bands between the 'in-plane' and the 'out-of-plane' Cu sites. The structures of two Cu atoms in the *xy*-plane and of those positioned along the *c*-axis are referred to them as the 'in-plane' and the 'out-of-plane' sites, respectively. The atomic positions of 'in-plane' and 'out-of-plane' sites are shown in the inset of Fig. 4. At high concentration of Cu, the t_2-state is located

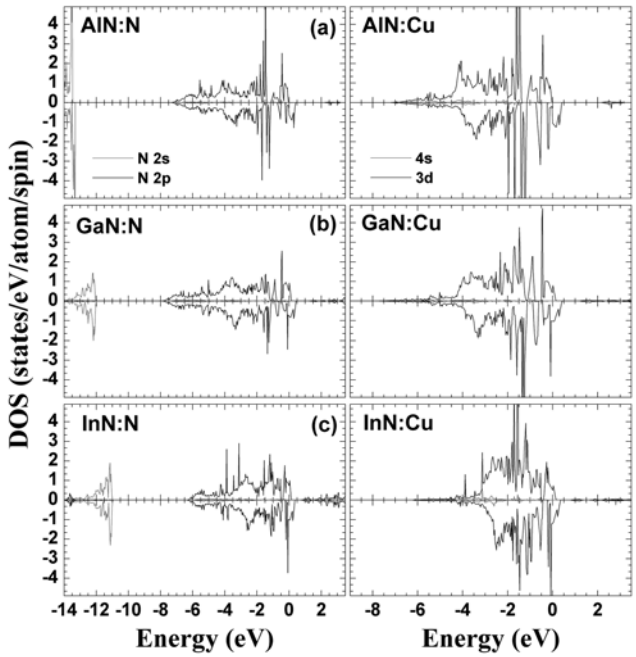

Fig. 3. Partial spin-polarized DOS of N and Cu in (a) Cu-doped AlN, (b) Cu-doped GaN, and (c) Cu-doped InN with the V_N and Cu concentration of 6.25%. The E_F is set to zero.

at the energy of E_F −1.5 eV. The *e*-states are dominant and strongly localized just below the E_F. The crystal field splitting between t_2 and *e* states in 'out-of-plane' Cu site of AlN is stronger than that of InN. When the concen-

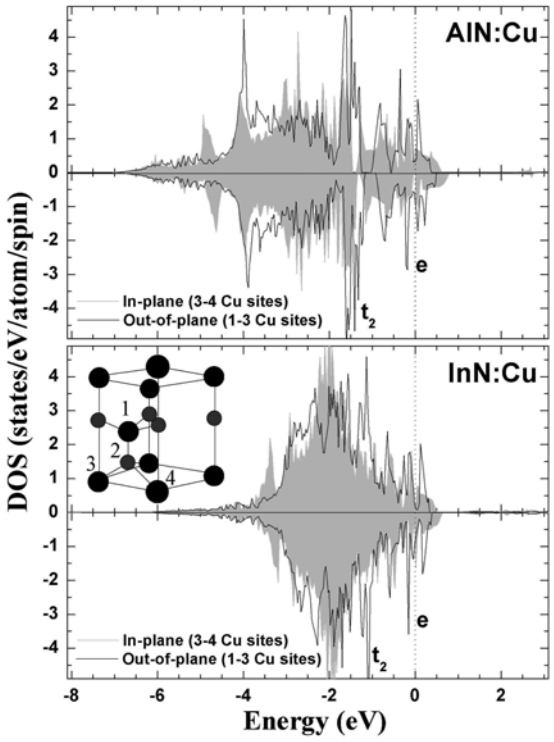

Fig. 4. Comparison between 'in-plane' (filled-gray) and 'out-of-plane' (solid-line) sites for partial spin DOS of Cu-3d in Cu-doped AlN and InN with the V_N and the Cu concentration of 12.5%. The E_F is set to zero. Wurtzite unitcell is shown in the inset. Number 1, 3, or 4 denotes the substituted Cu atom, number 2 denotes the V_N site, the 3-4 site represents the 'in-plane' Cu sites, and the 1-3 (or 1-4) site represents the 'out-of-plane' Cu sites.

tration of Cu increases in AlN or InN, the contribution in the ferromagnetism of *e*-levels is smaller than that of t_2-levels.

The Cu dopant orders ferromagnetically in the group III-nitrides. The ferromagnetic state is energetically more favorable than the nonmagnetic or antiferromagnetic state. As shown in Table 1, the Cu magnetic moments are 0.43, 0.25, and 0.19 μ_B, respectively, for AlN, GaN, and InN with the Cu concentration of 6.25%. When the Cu concentration increases, it is introduced the strong hybridization between N-2*p* and Cu-3*d* electrons to reduce the magnetic moment of Cu. For the 'in-plane' Cu site of 12.5%, the Cu magnetic moments are 0.19 and 0.13 μ_B for Cu-doped AlN and InN, respectively. For both Cu-doped AlN and InN, the substitution of Cu atom to the 'in-plane' site is energetically more favorable than that to the 'out-of-plane' site. These results are listed in Table 2.

The V_N site in AlN, GaN, and InN produces a repulsive potential pushing the conduction band into the band gap, and it produces an attractive defect potential attracting

Table 2. Substitution energy (E_s, in eV) for the 'in-plane' and the 'out-of-plane' $Al_{1-x}Cu_xN$ and $In_{1-x}Cu_xN$ ($x = 0.125$) with the V_N, total magnetic moments of supercell (M/cell, in μ_B). The values in the parenthesis represent the average magnetic moment of Cu atoms. The superscripts of (a) and (b) represent the 'in-plane' and the 'out-of-plane' sites, respectively.

	AlN		InN	
	E_s	M/cell	E_s	M/cell
$0.125^{(a)}$	−3.127	0.67(0.19)	−1.064	0.48(0.13)
$0.125^{(b)}$	−2.508	0.53(0.15)	−0.838	0.32(0.08)

levels of the valence state into the band gap. The defect site in AlN produces shallow acceptor states (E_v +0.2 eV). It induces the hybridization between the V_N state and Cu 3*d* states. The Cu magnetic moment is strongly reduced. The Cu 3*d*-Cu 3*d* coupling becomes weak. Therefore, the Cu magnetic moment is very low. In addition, the V_N site destroys the ferromagnetic coupling between the nearest neighboring two Cu atoms. The Cu dopant will combine easily with the site of V_N. Thus the control of N pressure plays important role in the design of high-performance devices.

4. Conclusion

We have systematically investigated the effects on the electronic and magnetic properties of N defect in clean or Cu-doped wurtzite III-nitrides by using the full-potential linear muffin-tin orbital method. For the Cu concentration of 6.25% and 12.5%, the ferromagnetic state is energetically more stable than the nonmagnetic and antiferromagnetic state. The site of N vacancy and the Cu dopant in AlN, GaN, and InN are strongly correlated. When there is a V_N site, the system doped two Cu atoms in the nearest neighboring sites is energetically more favorable than that without the V_N site. The Cu magnetic moment is strongly reduced due to the spin-exchange interaction between the Cu-3*d* and V_N states. When the Cu concentration increases in AlN, GaN, or InN, the Cu site combines with the V_N site easily. It may be formed a Cu+V_N state.

Acknowledgment

This work was supported by Konkuk University in 2011 (Dept. of Nano science and Mechanical engineering, Chungju).

References

[1] Q. Wang, A. K. Kandalam, Q. Sun, and P. Jena, Phys.

Rev. B **73**, 115411 (2006).
[2] X. Y. Cui, D. Fernandez-Hevia, B. Delley, A. J. Freeman, and C. Stampfl, J. Appl. Phys. **101**, 103917 (2007).
[3] S. G. Yang, A. B. Pakhomov, S. T. Hung, and C. Y. Wong, Appl. Phys. Lett. **81**, 2418 (2002).
[4] R. Frazier, G. Thaler, M. Overberg, B. Gila, C. R. Abernathy, and S. J. Peraton, Appl. Phys. Lett. **83**, 1758 (2003).
[5] X. Y. Cui, J. E. Medvedeva, B. Delley, A. J. Freeman, and C. Stampfl, Phys. Rev. B **75**, 155205 (2007).
[6] X. Y. Cui, J. E. Medvedeva, B. Delley, A. J. Freeman, N. Newman, and C. Stampfl, Phys. Rev. Lett. **95**, 256404 (2005).
[7] R. F. C. Farrow and S. S. P. Parkin, Appl. Phys. Lett. **87**, 172511 (2005).
[8] P. P. Chen, H. Makino, and T. Yao, J. Cryst. Growth **269**, 66 (2004).
[9] A. Ney, R. Rajaram, S. S. P. Parkin, T. Kammermeier, and S. Dhar, Phys. Rev. B **76**, 035205 (2007).
[10] M. Hashimoto, Y.-K. Zhou, M. Kanamura, and H. Asahi, Solid State Commun. **122**, 37 (2002).
[11] R. Q. Wu, G. W. Peng, L. Liu, Y. P. Feng, Z. G. Huang, and Q. Y. Wu, Appl. Phys. Lett. **89**, 062505 (2006).
[12] M. G. Ganchenkova and R. M. Nieminen, Phys. Rev. Lett. **96**, 196402 (2006).
[13] Y. Li, W. Fan, H. Sun, X. Cheng, P. Li, X. Zhao, and M. Jiang, J. Solid State Chem. **183**, 2662 (2010).
[14] S. Yu, Savrasov, Phys. Rev. B **54**, 16470 (1996) and references therein.
[15] B. S. Kang, W. C. Kim, Y. Y. Shong, and H. J. Kang, J. Cryst. Growth **287**, 74 (2006).
[16] Y. Wang and J. P. Perdew, Phys. Rev. B **43**, 8911 (1991).
[17] P. E. Blöchl, O. Jepsen, and O. K. Andersen, Phys. Rev. B **49**, 16233 (1994).
[18] C. G. Broyden, Math. Comput. **19**, 577 (1965).
[19] P. Pulay, Chem. Phys. Lett. **73**, 393 (1980).
[20] A. Zoroddu, F. Bernardini, and P. Ruggerone, Phys. Rev. B **64**, 045208 (2001).
[21] S.-H. Wei and A. Zunger, Appl. Phys. Lett. **69**, 2719 (1996).
[22] P. Rinke, M. Winkelnkemper, A. Qteish, D. Bimberg, J. Neugebauer, and M. Scheffler, Phys. Rev. B **77**, 075202 (2008).